REGULAR PAPER

Effect of protein aggregation on the spectroscopic properties and excited state kinetics of the LHCII pigment–protein complex from green plants

**Nikki M. Magdaong · Miriam M. Enriquez ·
Amy M. LaFountain · Lauren Rafka ·
Harry A. Frank**

Abstract Steady-state and time-resolved absorption and fluorescence spectroscopic experiments have been carried out at room and cryogenic temperatures on aggregated and unaggregated monomeric and trimeric LHCII complexes isolated from spinach chloroplasts. Protein aggregation has been hypothesized to be one of the mechanistic factors controlling the dissipation of excess photo-excited state energy of chlorophyll during the process known as non-photochemical quenching. The data obtained from the present experiments reveal the role of protein aggregation on the spectroscopic properties and dynamics of energy transfer and excited state deactivation of the protein-bound chlorophyll and carotenoid pigments.

Introduction

All photosynthetic organisms contain pigment–protein complexes that carry out energy transfer and electron transfer in implementing the process of photosynthesis (Hofmann et al. 1996; Blankenship 2002; Roszak et al. 2003; Liu et al. 2004; Frank and Cogdell 2012). Energy transfer is accomplished by light-harvesting (or antenna) complexes that absorb light in the visible region of the electromagnetic spectrum and transfer the energy to the reaction center protein which undergoes a series of oxidation–reduction reactions to convert the absorbed energy into electrical potential (Blankenship 2002).

Green plants contain two different reaction center proteins, photosystem I (PSI) (Witt et al. 1994; Fromme and Mathis 2004) and photosystem II (PSII), (Nelson and Yocum 2006) and many different light-harvesting proteins (Peter and Thornber 1991; Horton et al. 1999; Green and Parson 2003). The most abundant light-harvesting protein in green plants is the so-called LHCII complex (Fig. 1) which binds 14 chlorophyll (Chl) molecules non-covalently to the protein: eight Chl a and six Chl b (Kühlbrandt et al. 1994; Blankenship 2002; Liu et al. 2004; Telfer et al. 2008). Carotenoids are also found in the structure (Ruban et al. 1999; Croce et al. 1999; Blankenship 2002). These include two luteins that are arranged crosswise in the complex, one neoxanthin and one violaxanthin per monomeric unit (Kühlbrandt et al. 1994; Liu et al. 2004).

As photosynthetic organisms capture and convert light energy, the amount of energy absorbed but not channeled to the reaction center must be deactivated so that it does not lead to the photodestruction of the photosynthetic apparatus. This excess excitation energy may result in the formation of Chl triplet states which can sensitize the formation of singlet oxygen, a powerful oxidizing agent of Chl (Foote 1968; Foote et al. 1970; Krieger-Liszkay 2004). Carotenoid pigments protect photosynthetic organisms by quenching Chl triplet states (Frank and Cogdell 1996; Foyer and Harbinson 1999; Mozzo et al. 2008). Plants also dissipate excess energy prior to Chl triplet state formation and regulate the flow of energy to the reaction center (Demmig-Adams and Adams 1992; Horton et al. 1996;

N. M. Magdaong · M. M. Enriquez · A. M. LaFountain ·
L. Rafka · H. A. Frank (✉)
Department of Chemistry, University of Connecticut, U-3060,
55 North Eagleville Road, Storrs, CT 06269-3060, USA
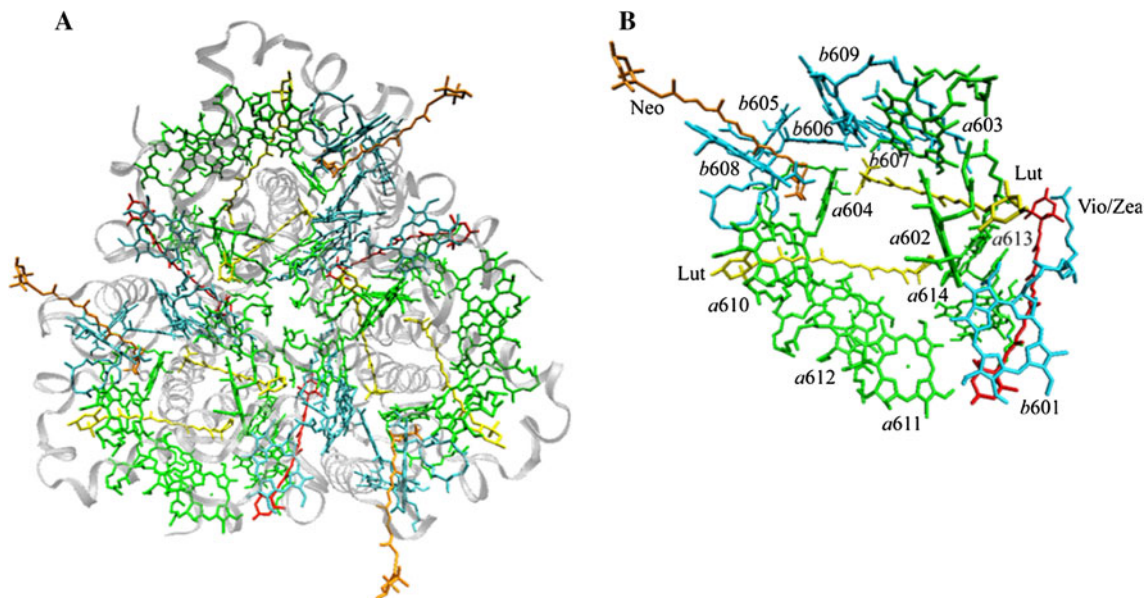e-mail: harry.frank@uconn.edu

Fig. 1 **a** Structure and arrangement of pigments in the LHCII trimer. **b** Each LHCII monomer subunit consists of eight Chl *a* (*green*), six Chl *b* (*cyan*), two lutein (*yellow*), one neoxanthin (*orange*), and one violaxanthin or zeaxanthin (*red*). The notation for the Chl pigments is taken from (Liu et al. 2004)

Müller et al. 2001; Holt et al. 2004; Avenson et al. 2008), but the mechanisms by which these processes occur are the subject of intense debate (Horton et al. 1999; Holt et al. 2004; Standfuss et al. 2005; Pascal et al. 2005; Amarie et al. 2007; Ruban et al. 2007). The dissipation of excess light energy is typically monitored by the extent to which Chl fluorescence originating from the light-harvesting pigment–protein complexes associated with PSII is quenched under different sample conditions (Horton et al. 1996; Phillip et al. 1996; Ruban et al. 1996). The overall process is called nonphotochemical quenching (NPQ) (Müller et al. 2001; Demmig-Adams and Adams 2002; Kulheim et al. 2002; Horton and Ruban 2005). NPQ has many different components (Müller et al. 2001), but the largest and most rapid component in green plants is the pH-dependent component known as qE.

At least four hypotheses have been advanced to explain the molecular basis of the qE component of NPQ. In one model, it is proposed to result from aggregation of the major trimeric LHCII complex which produces a conformational change that opens an energy transfer pathway to the lowest excited, S_1, state of a carotenoid for the deactivation of excess Chl-excited states (Pascal et al. 2005; Ruban et al. 2007). In a second model, energy from bulk Chls finds its way to a Chl/carotenoid heterodimer which undergoes charge transfer to form a carotenoid radical cation/Chl radical anion pair followed by subsequent charge recombination as the means of deactivating excess Chl *a* excited states (Holt et al. 2005; Ahn et al. 2008). Fleming and Niyogi et al. (Avenson et al. 2008; Cheng et al. 2008; Ahn

et al. 2008; Avenson et al. 2009) have reported that this process occurs solely in the minor Chl–protein complexes (Lhcb) and not in LHCII, whereas Kühlbrandt et al. (Barros and Kuhlbrandt 2009; Barros et al. 2009) have proposed that carotenoid radical cation formation is facilitated by the binding of a separate protein, the PsbS complex (Niyogi et al. 2005), with either LHCII or an Lhcb subunit. A third model proposes that carotenoid/Chl exciton coupling provides a pathway for deactivation of excess excited Chl via the rapidly decaying S_1 state of a carotenoid (Bode et al. 2008, 2009; Liao et al. 2010). A fourth model requires oligomerization or aggregation of LHCII trimers to form Chl/Chl exciton pairs that undergo charge transfer as the pathway for Chl-excited state deactivation (Miloslavina et al. 2008; Holzwarth et al. 2009; Muller et al. 2010).

In the present work, the effect of aggregation of the LHCII pigment–protein complex on the spectroscopic properties and dynamics of the bound pigments is examined. Many reports of fluorescence quenching induced by aggregation of the LHCII complex have appeared (Bassi et al. 1991; Mullineaux et al. 1993; Gilmore et al. 1995; Vasil'ev et al. 1997; Moya et al. 2001; Palacios et al. 2002; Huyer et al. 2004; Pascal et al. 2005; van Oort et al. 2007), but the issue of whether aggregation plays a role in facilitating quenching of Chl-excited states in vivo has yet to be fully addressed. It should be emphasized that although aggregation of pigment–protein complexes has been implicated in at least one of the mechanisms seeking to explain NPQ, aggregating randomly dispersed LHCII in vitro may lead to the pigment–protein complex being

arranged in orientations different from those achieved when the complex is constrained by the two-dimensional structure of the photosynthetic membrane in which it is naturally bound. Nevertheless, the studies presented here and elsewhere (Nordlund 1981; Ide et al. 1987; Pieper et al. 1999a; Andreeva et al. 2009; Johnson and Ruban 2009; van Oort et al. 2011; Ilioaia et al. 2011a; Gruszecki et al. 2012) on aggregated monomeric and trimeric LHCII are assessing how much quenching occurs when the protein forms aggregates and what molecular factors control the process of Chl fluorescence quenching. In addition, the changes in the energy transfer rates and efficiencies that result from protein aggregation will help understand the behavior of closely associated LHCII pigment–protein complexes in vivo.

Materials and methods

Preparation of LHCII complexes

LHCII trimers were prepared from spinach leaves using previously described procedures (Das and Frank 2002). Thylakoid membranes were isolated from spinach leaves and further resuspended and solubilized to obtain BBY particles (Berthold et al. 1981). Sucrose density gradient ultracentrifugation was employed to separate the components of BBY. The second band from the top contained the monomeric LHCII and CP complexes while the third band contained the trimeric LHCII complex. LHCII trimers were further purified by a second sucrose density gradient ultracentrifugation step, dialyzed against buffer containing 10 mM HEPES, 0.06 % n-dodecyl-β-D-maltoside (β-DM), pH 7.6, and stored at -80 °C.

Monomeric LHCII was separated from the CP complexes using the isoelectric focusing (IEF) protocol described previously (Das and Frank 2002) but with slight modifications. 100 mL of slurry was prepared and contained 5 % (w/v) Sephadex G-100, 2 % (w/v) Pharmalyte carrier ampholytes (pH 2.5–5.0), 1 % (w/v) glycine, 0.06 % (w/v) β-DM, and distilled water. Six IEF electrode strips were cut into 10.5 cm lengths and soaked in 2 % (w/v) Pharmalyte solution. The strips were then placed on both ends of the Pharmacia Multiphor II Electrophoresis system gel tray (26.0 cm × 11.0 cm). The slurry was slowly poured onto the tray and allowed to form a homogenous layer. Air bubbles were removed carefully and the tray with the slurry was placed on a balance below approximately 50 cm of a small fan. $\sim$17–18 g of water was allowed to evaporate over a period of 2 h. Anode and cathode strips were placed on top of the electrode strips prepared by soaking strips in either 1 M phosphoric acid (anode solution) or 1 M sodium hydroxide (cathode

solution). To insure thermal conductivity between the cooling plate and the gel tray, a 0.1 % (v/v) solution of Triton X-100 was applied to the cooling plate. The gel was pre-focused for 1 h at 8.0 W with the temperature maintained at 4 °C. 1 mL of band 2 containing the PS II antenna complexes from the previous sucrose density gradient ultracentrifugation step was mixed with 1 mL of deionized water and 0.5 mL of 3 % β-DM. The mixture was then kept on ice and stirred occasionally for 30 min before centrifugation at 12,000×g for 5 min at 4 °C using a Sorvall SS-34 rotor. $\sim$2.0 mL of the supernatant was mixed with the gel scraped out using a 10 × 2 cm sample applicator applied at about 2 cm from the cathode. The sample slurry was then poured back into the sample applicator and the applicator removed after which time the sample was allowed to equilibrate hydrostatically for $\sim$3 min. The focusing was continued for 15 h at a constant power of 8.0 W, 4 °C. The green bands observed after the completion of the focusing were separated using a fractionating grid frame, collected using a spatula, and eluted in PEGG elution columns using a minimum amount of buffer which contained 100 mM HEPES and 0.06 % β-DM at pH 7.6. Prior to elution, a small amount of each band was dissolved in deionized water and the isoelectric point (pI) was measured using a microelectrode. Carrier ampholytes and sucrose were removed from the sample by dialysis against buffer containing 10 mM HEPES, 0.02 % β-DM at pH 7.6. LHCII monomers were then frozen at -80 °C until used in the spectroscopic experiments.

Aggregated LHCII complexes were prepared using Bio-Beads (Bio-Rad 152-8920), which upon addition to the solution, reduce the β-DM concentration (Ruban et al. 2007). This was accomplished by adding 200 mg of beads/mL to the LHCII sample and stirring in the dark at room temperature for approximately 15 min.

Pigment analysis

The pigment composition of the LHCII complexes was confirmed by extraction using 50/50 (v/v) acetone/methanol and by HPLC analysis as follows: Approximately 1 mL of the LHCII complex was dialyzed against 1 L of 10 mM HEPES buffer, pH 7.6 (without β-DM detergent) for 24 h at 4 °C. The dialyzed sample was then placed in a 1.5 mL Eppendorf tube having small holes at the top and lyophilized for 48 h. After lyophilization, the sample was redissolved in 50/50 (v/v) HPLC grade acetone/methanol and dried under a stream of nitrogen. The dried sample was then taken up in acetonitrile, which was the HPLC injection solvent, and filtered through a Millex microsyringe (0.2 μm). The HPLC solvents were: solvent A consisting of 87 % acetonitrile, 10 % methanol, and 3 % water; and

solvent B consisting of 100 % ethyl acetate. All solvents were HPLC grade and purchased from Fisher Scientific. The HPLC protocol was programed for a flow rate of 1 mL/min and was isocratic for the first 15 min using 99 % solvent A and 1 % solvent B. Then, a linear gradient was applied over 25 min until the solvent composition was 60 % solvent A and 40 % solvent B. This solvent composition was maintained for the remaining 20 min of the protocol (See Online Resource 1, Fig. S1, for a representative HPLC trace).

Steady-state spectroscopic methods

A Varian Cary 50 UV/Vis spectrophotometer was used to obtain steady-state absorption spectra. For the steady-state fluorescence measurements, a Jobin–Yvon Horiba Fluorolog-3 Model FL3-22 fluorimeter having double emission and excitation monochromators, 1,200 grooves/mm gratings, a Hamamatsu R928P PMT detector, and a 450 W Osram XBO xenon arc lamp were used. The emission spectra of LHCII samples were obtained with a sample OD of 0.05 at the 640 nm excitation wavelength. The bandpass settings were 2 and 1 nm, for the excitation and emission monochromators, respectively. The fluorescence excitation spectra of the samples were recorded with the emission wavelength set to 700 nm and the bandpass settings were 2 and 4 nm, for the excitation and emission monochromators, respectively. For spectroscopic experiments on LHCII samples at cryogenic temperatures, a mixture of glycerol and 10 mM HEPES buffer, pH 7.6 was added to the samples to a final concentration of 70 % (v/v) glycerol in plastic cuvettes (Plastibrand model no. 759150).

For absorption and fluorescence experiments at 77 K, a custom made optical immersion Dewar cryostat was used to hold the samples. The cuvette containing the sample was secured into a sample holder and lowered slowly into the cryostat containing liquid nitrogen. For the experiments below 77 K, the sample was placed in a cryostat (Janis Model STVP-100-1) and liquid helium was introduced via a transfer arm (Janis ST-LINE).

Time-resolved fluorescence spectroscopy

Time-resolved fluorescence spectra of the LHCII samples were obtained using Jobin–Yvon Horiba Fluorolog-3 Model FL3-22 fluorimeter with a time-correlated single-photon counting (TCSPC) module and a pulsed NanoLED-670L diode generating 665 nm light with a <200 ps pulse duration as excitation light source. Lifetimes and amplitudes were extracted by fitting the time response data detected at 680 nm using a sum of exponentials function.

Femtosecond time-resolved transient absorption spectroscopy

Room temperature transient absorption spectroscopy experiments were performed using the femtosecond transient absorption spectrometer setup previously described (Ilagan et al. 2005; Fuciman et al. 2012). The optical densities (OD) of the LHCII samples were adjusted to 0.4–0.6 at the excitation wavelength in a cuvette with 2 mm path length. Excitation of the samples was achieved by tuning the pump beam to either 490 nm which excited the S_2 state of the carotenoids and the Soret band of Chl b or to 677 nm which excited the Q_Y band of Chl a. The measurements were averaged over 5 s. The pump beam had 1.2 μJ/pulse energy in a 1 mm diameter spot size, which corresponded to 3.8×10^{14} and 5.2×10^{14} photons/cm^2 pulse intensity at 490 and 677 nm excitation, respectively. In order to prevent photodegradation, the samples were continuously mixed using a magnetic microstirrer and the absorption spectra before and after transient absorption experiments were taken to assess sample integrity.

Results and discussion

Steady-state absorption and fluorescence spectroscopy

The absorption spectra of the LHCII monomers, trimers, and aggregates taken at room temperature and 10 K are presented in Fig. 2. As can be seen in the figure, and especially in the insets which emphasize the Q_Y region of Chl a and b absorption between 600 and 700 nm, aggregation leads to only very small changes in the absorption spectral features of the complexes. Lowering the temperature to 10 K results in more structured and resolved spectra compared to those seen at room temperature. Also, at any given temperature, the absorption spectra in the Q_Y region of the aggregated LHCII proteins were slightly broader, and in the case of aggregated trimers, the maximum absorption in this region was also slightly red-shifted by 1 nm, compared to those of the unaggregated proteins.

In contrast to the minimal effect of protein aggregation on the absorption spectra, the effect on the emission spectral intensities and lineshapes is striking (Naqvi et al. 1997; Ruban et al. 1997; Barzda et al. 2001; Gruszecki 2006). Figure 3 shows that ∼15 min after addition of the Bio-Beads to the samples which promotes protein aggregation, the fluorescence intensity is reduced substantially. Aggregation of the monomers and trimers reduced the fluorescence emission intensity by 93 and 91 %, respectively (Fig. 3). By comparison, the exact same samples exhibited only a 17 and 5 % change, respectively, in the intensity of their absorption spectra (Fig. 3). This indicates that the large reduction in fluorescence intensity cannot be attributed to

Fig. 2 Overlay of the steady-state absorption spectra of LHCII complexes (*black line*) and aggregates (*red line*) at room and cryogenic temperatures. *Insets* show an expanded view of the Q_Y absorption region between 625 and 700 nm
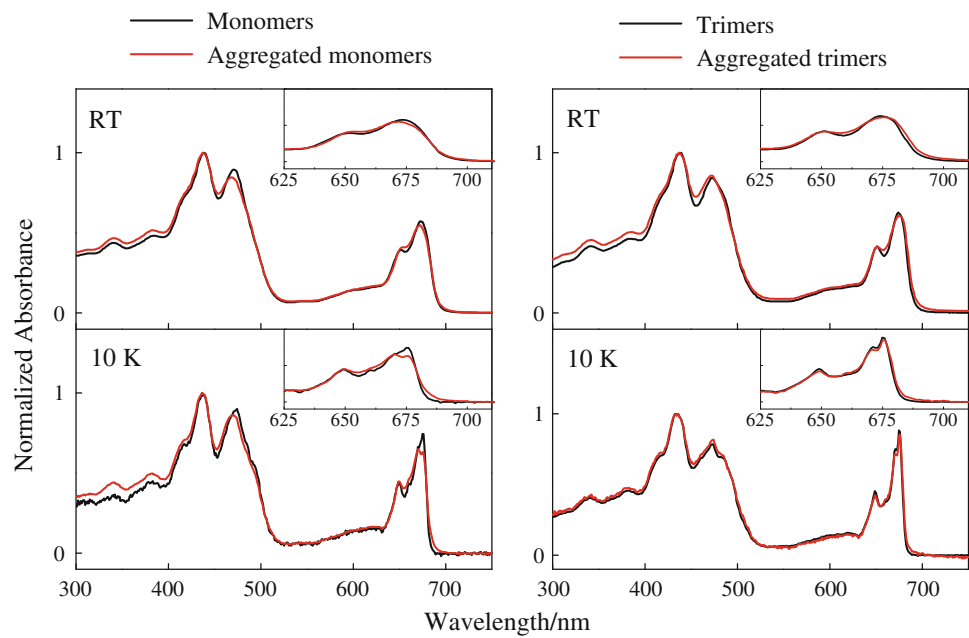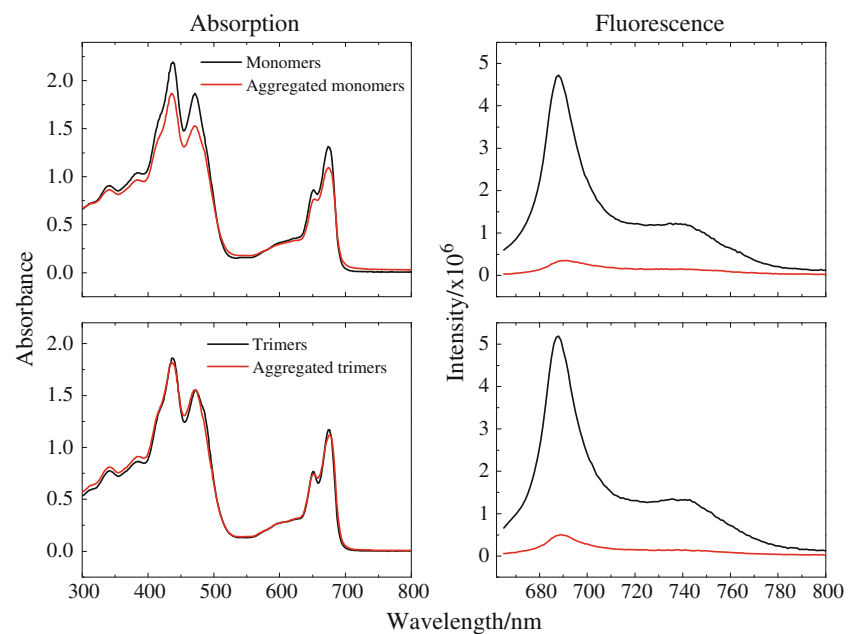

Fig. 3 Effect of aggregation on the absorption and fluorescence spectra of LHCII monomers and trimers. The spectra of the aggregated monomers was taken ~20 min following the addition of the biobeads, and that of the aggregated trimers was taken after ~10 min


protein precipitation or degradation. 30 minutes after the addition of the Bio-Beads, the emission intensity reached a constant level that was approximately an order of magnitude less than that of its initial value.

As has been reported previously (Ruban et al. 1995, 1997; Andreeva et al. 2009), there is also a substantial difference in the emission spectral lineshapes of the aggregated versus unaggregated LHCII samples taken at various temperatures (Fig. 4). For the unaggregated monomers, at room temperature, the maximum intensity appeared at 682 nm. As the temperature was lowered to 80 K, the maximum blueshifted to 679 nm, where it remained as the temperature was

further lowered to 10 K. Also, as the temperature was lowered, the spectra became more intense and narrower. The 10 K spectrum had a full-width at half-maximum (FWHM) of 7 nm and was noticeably sharper than the room temperature spectrum which had a FWHM of 18 nm (Fig. 4).

For the aggregated monomers at room temperature, the emission band maximum appeared at 681 nm (Fig. 4). As the temperature was lowered to 80 K, the spectrum increased in intensity, broadened noticeably to a FWHM of 23 nm, and a shoulder appeared on the long wavelength side of the major band. When the temperature was lowered to 10 K, the spectrum gained even more in intensity and,

Fig. 4 Temperature dependence of the steady-state emission spectra of LHCII complexes after excitation at 640 nm. Samples were adjusted to have the same absorption at the excitation wavelength
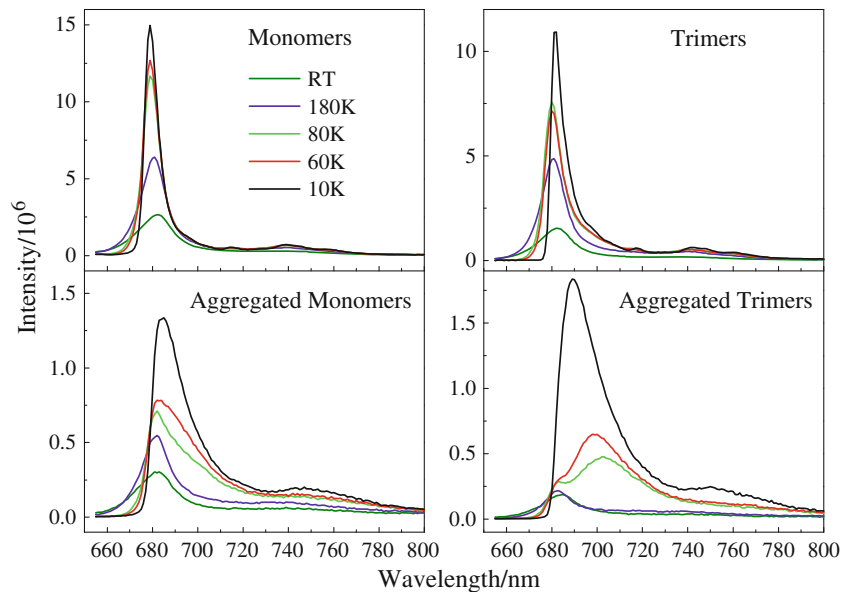
unlike the spectrum of the unaggregated monomers which narrowed as the temperature was lowered, remained very broad with a FWHM of 18 nm. Also, its maximum at this temperature was red-shifted relative to that of the unaggregated monomers and appeared at 685 nm.

For the unaggregated trimer sample at room temperature, the maximum intensity appeared at 682 nm just like the unaggregated monomer sample. As the temperature was lowered to 80 K, the maximum blue-shifted slightly to 680 nm. At 10 K, the maximum shifted back to 682 nm. Also like the monomeric sample, as the temperature was lowered, the spectrum became more intense and narrower. The FWHM for the unaggregated trimer spectrum at 10 K was 7 nm, whereas at room temperature it was 17 nm.

For the aggregated trimers at room temperature, the emission band maximum was red-shifted to 685 nm compared to 682 nm for the unaggregated trimers at the same temperature. As the temperature was lowered to 80 K, the spectrum increased in intensity and split into two noticeable bands having maxima at 683 and 703 nm. When the temperature was lowered further to 10 K, the spectrum continued to increase in intensity, but it coalesced into a single major broad band having a maximum at 689 nm and a FWHM of 21 nm. It is important to note that for both the monomer and trimer LHCII samples, the 10 K emission spectra of the aggregated proteins were substantially broader than those of the unaggregated samples. Also, in all cases a minor low-energy vibronic emission band appeared between 740 and 750 nm.

As control samples and for use in interpreting the effect of protein binding and aggregation on the Chl emission profiles, the fluorescence spectra of purified Chls *a* and *b* in 2-MTHF were recorded as a function of temperature (Fig. 5). From room temperature to 10 K the FWHM of the Q_Y band of the emission spectrum of Chl *a* was found to be
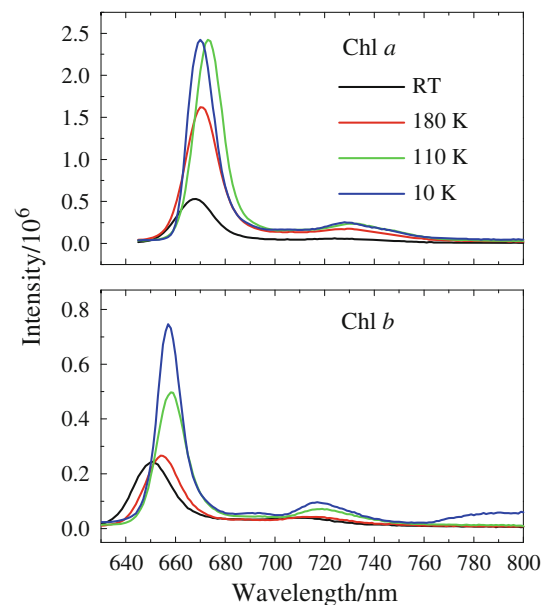

Fig. 5 The effect of temperature on the fluorescence spectra of purified Chl *a* (*top*) and Chl *b* (*bottom*)

only very slightly narrower by ∼1 nm than that of Chl *b*. Also, as the temperature was lowered from room temperature to 10 K, the maximum in the emission spectrum of Chl *a* shifted from 668 to 670 nm. For Chl *b*, there was also a noticeable shift in the band maximum from 651 nm at room temperature to 657 nm at 10 K.

Fluorescence excitation spectroscopy

Figure 6 shows the excitation spectra of the LHCII unaggregated and aggregated monomeric and trimeric proteins monitored at 700 nm overlaid with their respective $1 - T$ spectra,

Fig. 6 Excitation spectra (*black lines*) overlaid with $1 - T$ spectra (*red lines*) of LHCII complexes at room and cryogenic temperatures. Excitation spectra were monitored at 700 nm. The intensities were normalized at the Chl a Q_Y band maximum
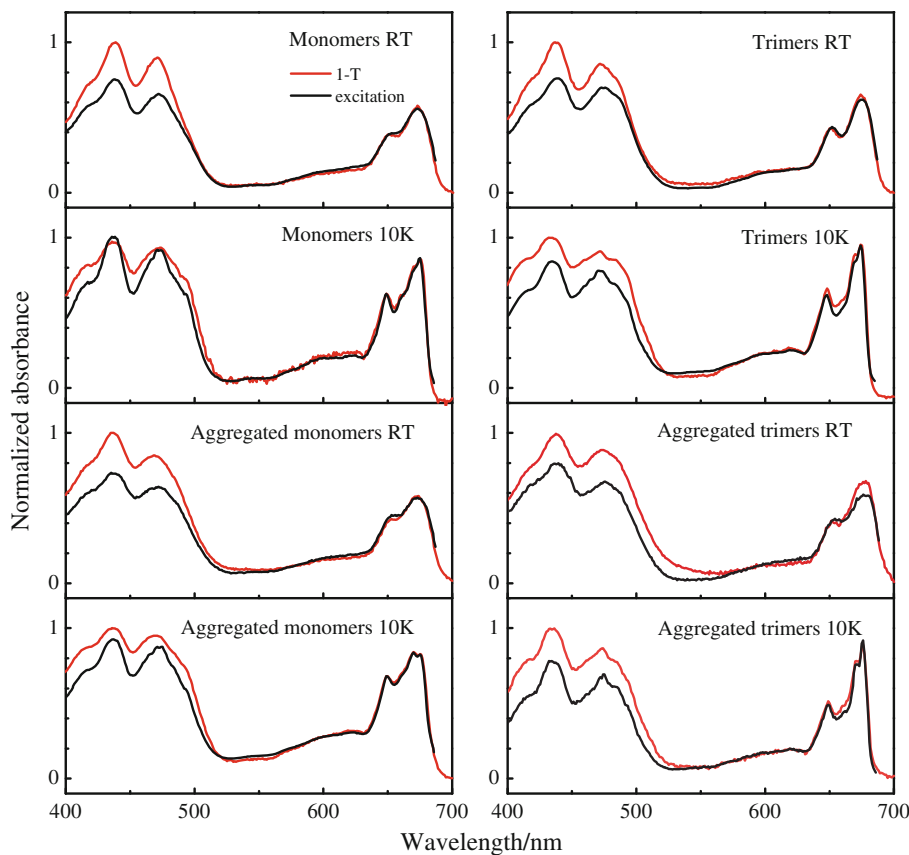
where T is transmittance. The spectra show a difference in intensity between the $1 - T$ and excitation spectra primarily in the carotenoid absorption region between approximately 400 and 520 nm indicating that energy transfer from the carotenoids to Chl a is not 100 % efficient. This is consistent with previous reports (Gradinaru et al. 2000; Croce et al. 2001; Frank et al. 2001; Das and Frank 2002). However, for the monomeric LHCII complexes (left four panels in Fig. 6), the excitation spectra in this region match the $1 - T$ spectra better at low temperatures than at room temperature regardless of whether the complexes are aggregated or not. This indicates that as the temperature is lowered, the efficiency of energy transfer from the carotenoids to Chl a is enhanced. This is not the case for the trimeric complexes (right four panels in Fig. 6) where the efficiency of carotenoid-to-Chl a energy transfer remains constant at $\sim$70 %. For all the samples, whether monomeric or trimeric, aggregated or unaggregated, the agreement between the excitation and $1 - T$ spectra in the region of the Chl b Q_Y band near 640 nm is excellent indicating a high efficiency of energy transfer from Chl b to Chl a.

Fluorescence kinetics

The effect that aggregation of the LHCII complexes had on the kinetics of decay of Chl a fluorescence was investigated using

time-correlated single-photon counting spectroscopy. Figure 7 shows the results of monitoring the time course of Chl a fluorescence decay probed at 681 nm following excitation into the Chl b Q_Y band at 665 nm. It is seen in Fig. 7 that the Chl a fluorescence decay time of unaggregated monomeric and trimeric LHCII are essentially the same. However, aggregation of the monomeric and trimeric LHCII complexes leads to significantly faster deactivation of Chl a excited states with the aggregated trimers decaying approximately 50 % faster than the aggregated monomers (compare blue and red traces in Fig. 7). The results also show that aggregating monomeric LHCII complexes does not lead solely to trimeric LHCII or to aggregated LHCII trimers, but instead has its own Chl fluorescence quenching characteristics.

In order to gain a better understanding of the kinetic components responsible for the Chl a fluorescence decay, the time-resolved data were globally fit to a sum of exponentials function which produced decay-associated spectra (DAS). These are shown in Fig. 8. The fluorescence kinetics from all of the samples can be accounted for by three decay components which for the unaggregated LHCII monomers and trimers (top two panels in Fig. 8) fall within the ranges of 0.21 ± 0.4, 3.3 ± 0.1, and 4.9 ± 0.5 ns which are very similar to what was reported previously using picosecond time-resolved fluorescence on Chl-a/b protein complex at room temperature (Ide et al. 1987). The DAS from these two
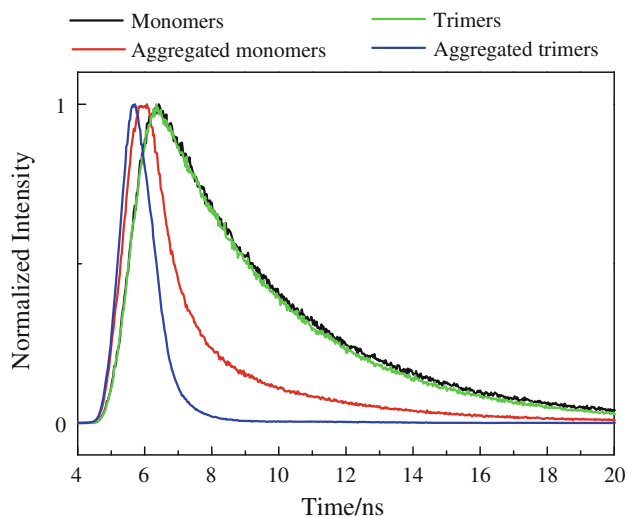
Fig. 7 Time-resolved fluorescence decay profiles of LHCII complexes excited at 665 nm and probed at 681 nm at room temperature

samples all have very similar lineshapes with only minor wavelength shifts. The first and fastest component has a maximum in the range 677 ± 2 nm and very likely corresponds to unequilibrated Chl *a* excitation. The second and third components have maxima that are slightly red-shifted to 682 ± 1 and 679 ± 2 nm, respectively and based on previous work (Ide et al. 1987; Frank et al. 2001; Andersson et al. 2001) can be assigned to the decay of the vibrationally equilibrated lowest excited singlet state of Chl *a* in different protein environments.

Aggregation of the monomeric LHCII complex slightly increases the lifetime of the fastest component (square symbols in the two left hand panels of Fig. 8) and decreases the lifetimes of the two long-lived components by a moderate amount (circle and triangle symbols in the two left hand panels of Fig. 8). The more important observation is that upon aggregation, the fastest component (square symbols in the two left hand panels of Fig. 8) increases in amplitude by nearly a factor of four and red-shifts by ∼7 nm, whereas the amplitudes of the two longer-lived components decrease by a factor of ∼3 and their wavelength maxima remain relatively unchanged. Aggregation of the trimeric LHCII complex leads to even more dramatic changes in the DAS profiles and lifetimes of the components. The fastest component observed in the aggregated trimers has a unique band at ∼687 nm which may represent the deactivation of a rapidly populated low-energy excitation trap. Also remarkable is the observation that the amplitude of the slowest component has been diminished by an order of magnitude relative to that observed in the unaggregated trimer sample. These kinetic results are entirely consistent with the steady-state fluorescence experiments (Fig. 3) which revealed that the aggregated monomer and trimer samples were both ∼90 % quenched with respect to the unaggregated samples. However, the more interesting aspect in comparing the lifetimes of the kinetic components of the aggregated monomers and trimers is the qualitative differences observed between these two forms of the LHCII protein.

Fig. 8 Decay associated fluorescence spectra of the LHCII complexes taken using 665 nm excitation at room temperature as described in the text. All of the samples were measured at the same total Chl concentration
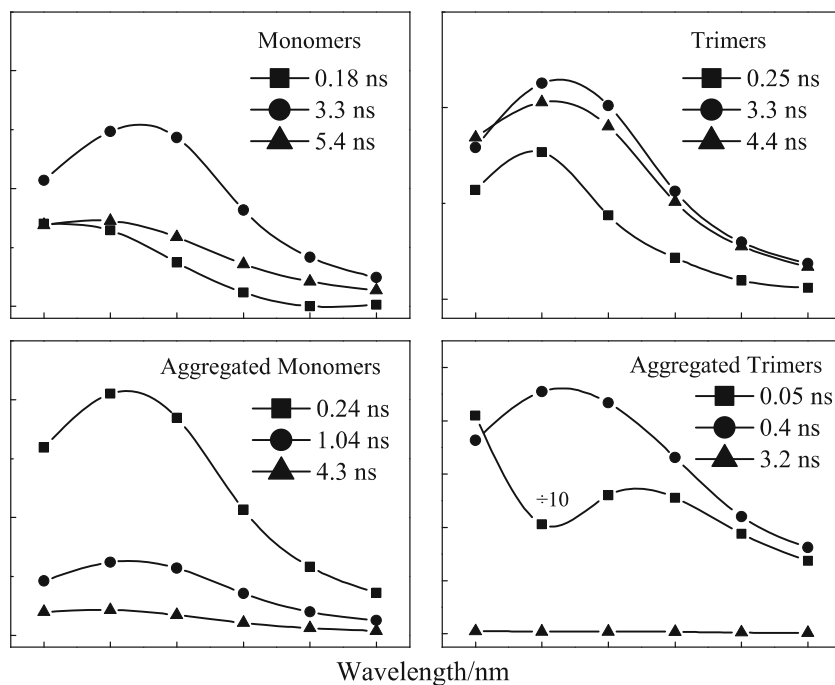
Transient absorption

Transient absorption spectra of the monomeric and trimeric, aggregated and unaggregated LHCII complexes taken at various delay times after laser excitation are presented in Fig. 9. Spectra in the visible region recorded upon excitation at 490 nm (left hand column in Fig. 9) show that essentially within the time profile of the excitation laser pulse, there occurs an onset of bleaching of the carotenoid bands in the region 450–525 nm, a bleaching of the Chl a and b Q_Y absorption bands at ~ 685 and ~ 650 nm, respectively, and a buildup of carotenoid $S_1 \rightarrow S_N$ transient absorption between 500 and 600 nm. In all of the samples, the carotenoid transient absorption signal decreases by about 30 % and the Chl b Q_Y band bleaching decreases by approximately 90 % in 5 ps (see green traces in the left hand panels of Fig. 9). However, the kinetics of the recovery of the Chl a Q_Y band bleaching depend on the aggregation state of the LHCII complex. The recovery is much faster for the aggregated monomers and trimers compared to the unaggregated complexes. This is evidenced by the fact that at 500 ps, the bleaching of the

Chl a Q_Y band in the aggregated complexes is completely gone (see the blue traces in the second and fourth panels on the left hand side of Fig. 9), indicating that all the Chl a molecules have returned to the ground state within this time frame. However, for the unaggregated monomers and trimers, a significant amount of bleaching of the Chl a Q_Y band persists in the transient spectra taken at 500 ps (see the blue traces in the first and third panels on the left hand side of Fig. 9). This indicates that many Chl a molecules are remaining in the excited state well beyond 500 ps.

Transient NIR spectra recorded upon 490 nm excitation show a fast-decaying carotenoid signal between 900 and 1,200 nm presumably associated with the $S_2 \rightarrow S_N$ transition (see the black traces in the second column of panels in Fig. 9). The transient absorption feature at ~ 910 nm appears slightly sharper in the monomeric complexes, but otherwise the spectra taken at this delay time and at 300 fs and 50 ps are very similar for all the complexes. Transient NIR spectra recorded after exciting the samples directly into the Q_Y band of Chl a with 677 nm light (see the fourth column of panels in Fig. 9) display features that are not sufficiently distinct from each other to draw any significant
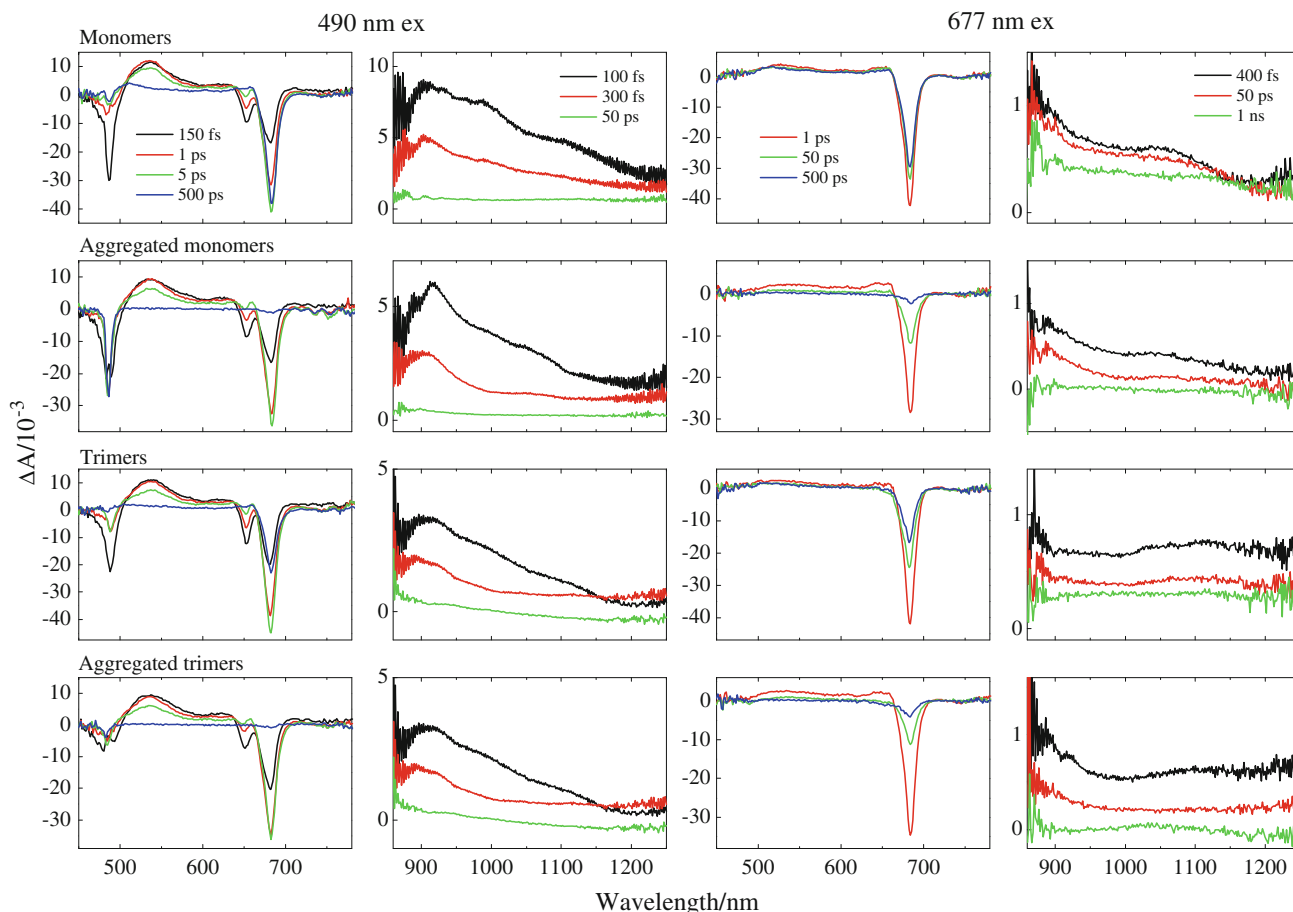

Fig. 9 Transient absorption spectra of LHCII complexes in the visible and NIR regions. The spectra were recorded at the indicated delay times after excitation at 490 and 677 nm

conclusions regarding the differences between the monomers and trimers, or aggregated and unaggregated LHCII complexes.

Spectra taken at 1 ps in the visible region after 677 nm excitation directly into the Chl a Q_Y band (third column in Fig. 9) show a pronounced bleaching of this band, but also display a weak positive signal in the spectral region between 480 and 600 nm which is much more noticeable for the aggregated complexes compared to the unaggregated complexes (see the red traces in the third column of panels in Fig. 9). The maxima in the weak positive signals for the aggregated monomers and trimers correspond precisely to the position of the $S_1 \rightarrow S_N$ transitions seen upon 490 nm excitation (first column of panels in Fig. 9). This suggests that upon excitation into the Q_Y band of Chl a at 677 nm, there is some energy transfer from Chl a to the S_1 state of a carotenoid which then rapidly deactivates to the ground state as a mechanism for quenching. The weak intensity of the carotenoid transient absorption signal supports the kinetic model for quenching proposed by Ruban et al. (2007) whereby a relatively slow rate of energy transfer from Chl a to a carotenoid is followed by fast deactivation of the excited state energy to the ground state by the carotenoid. At 50 ps, the weak positive signal has disappeared, but the Chl a Q_Y band bleaching persists albeit to a lesser extent than seen at 1 ps. By 500 ps, the Chl a Q_Y band bleaching is greatly diminished in the aggregated LHCII samples (see the blue traces in the second and fourth panels in the third column of Fig. 9), indicating that almost all the Chl a molecules have returned to the ground state. This is not the case for the unaggregated LHCII samples (see the blue traces in the first and third panels in the third column of Fig. 9) where the Chl a band bleaching is still substantial. This indicates once again that for the aggregated complexes there is a rapid pathway for deactivation of excited Chl a, but for the unaggregated complexes, many Chl a molecules are remaining in the excited state well beyond 500 ps.

The profound differences in the kinetics of Chl a excited state relaxation among the complexes is further illustrated by the time traces shown in Fig. 10. Upon excitation at 490 nm and monitoring the recovery of the Chl a Q_Y band bleaching, monomeric LHCII decays relatively slowly (in ~3 ns) back to the ground state. Trimeric LHCII undergoes a multiphasic recovery where part of the population decays rapidly in ~25 ps, presumably due to exciton annihilation owing to close proximity between pigments in the trimeric system, and the remaining excited states population decays in ~1 ns. Both aggregated monomers and trimers deactivate much faster (~120 ps) than the unaggregated systems consistent with the observation of extensive Chl a excited state quenching seen in the fluorescence experiments (Figs. 3, 7, 8).
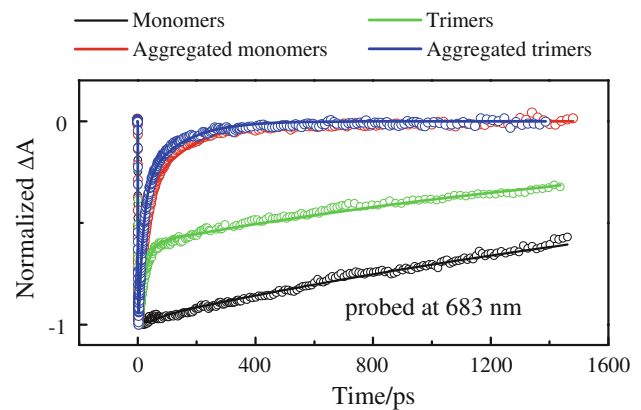
Fig. 10 Transient absorption decay profiles monitored at 683 nm in the Q_Y region of Chl a absorption upon 490 nm excitation at room temperature

In order to obtain a more detailed understanding of the dynamics of energy transfer and excited state deactivation, the spectral and temporal datasets from the transient absorption experiments recorded in the visible and NIR regions using either 490 or 677 nm excitation were globally fit according to a sequential excited state decay model. The analysis yielded evolution associated differential spectra (EADS) (van Stokkum et al. 2004) that characterize the excited state energy transfer pathways and decay components of the carotenoids and Chls bound in the LHCII complexes. The results of the analysis are presented in Fig. 11, and the lifetimes of the components obtained from the fits to the data are given in Table 1. For the experiments using 490 nm excitation, five kinetic components were required to obtain a satisfactory fit to the data taken either in the visible or NIR regions (see the left hand columns panels of Fig. 11 and see Online Resource 2, Fig. S1). The EADS traces generated from the NIR transient absorption data are provided in the Online Resource as Fig. S2 from which it can be seen that the traces are very similar for all the complexes. Hence, the emphasis here will be on the EADS results generated from the transient spectra recorded in the visible region.

From Fig. 11, it can be seen that the fastest EADS component (black traces in the left hand column panels) decayed in ≤110 fs with the lifetime of this component being approximately 20 % faster for the aggregated samples versus the unaggregated complexes. In fact, all of the EADS components obtained from the aggregated complexes have shorter lifetimes than the corresponding components from the unaggregated samples (Fig. 11; Table 1). The first EADS component displayed spectral features in the visible region that can be assigned to a bleaching of the carotenoid $S_0 \rightarrow S_2$ transition as well as bleaching of the Chl a and b Q_Y bands. Carotenoids and Chl b are both directly excited by 490 nm light which explains the
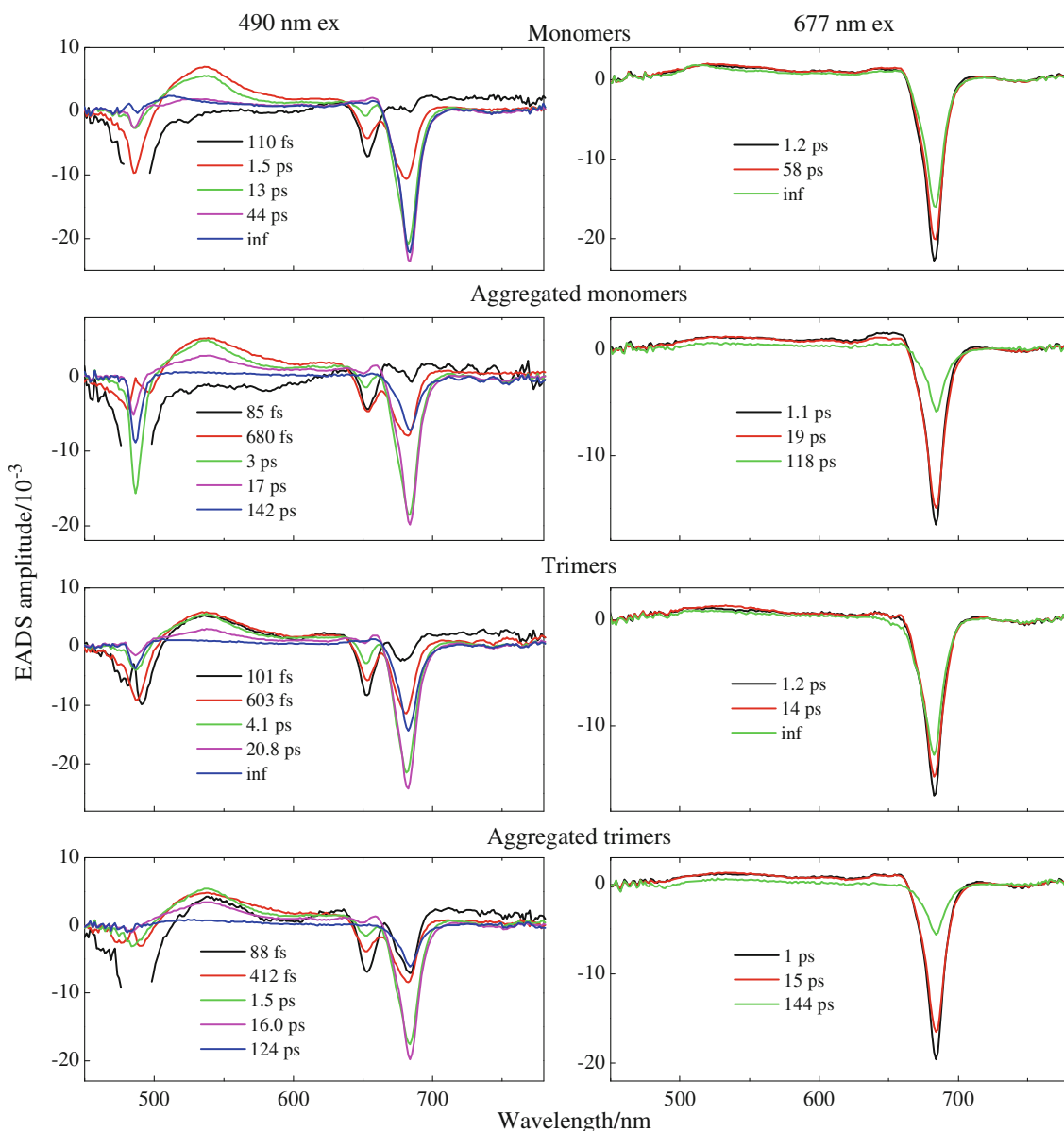
Fig. 11 Evolution associated difference spectra (EADS) of unaggregated and aggregated LHCII complexes obtained from global fitting the transient absorption datasets recorded in the visible region using 490 and 677 nm excitation

immediate onset of the bleaching of these pigments. However, because Chl a does not absorb at this excitation wavelength, no bleaching of the Q_Y band of Chl a is expected unless there is very rapid energy transfer to Chl a from either the S_2 state of the photoexcited carotenoids or Chl b. Indeed, very little bleaching of the Chl a Q_Y band appears in this EADS component from either the aggregated or unaggregated monomeric LHCII samples (black traces in the top left two panels of Fig. 11). However, Chl a Q_Y band bleaching is seen in the first EADS component of both the aggregated and unaggregated trimeric LHCII samples (black lines in the bottom left two panels of Fig. 11), with the bleaching being more pronounced for the

aggregated trimers. There is clear evidence of rapid energy transfer to Chl a from either the S_2 state of the carotenoids or Chl b, and apparently, this route of energy transfer is facilitated by the formation of the trimeric LHCII structure from monomeric subunits.

In going from the first to the second EADS component, in all cases, there is a decrease in the bleaching of the $S_0 \rightarrow S_2$ transition of the carotenoids and a substantial increase in the bleaching of the Chl a Q_Y absorption band (see the red traces in the left hand column of Fig. 11). Also, the bleaching of the Chl b Q_Y absorption band at ∼650 nm either remains the same (aggregated monomers) or decreases (all other complexes). This indicates that no

Table 1 Dynamics of the excited states of LHCII monomers, trimers, and aggregates

LHCII sample	Excitation λ (nm)	Probe region	Lifetime (ps)				
			τ_1	τ_2	τ_3	τ_4	τ_5
Monomers	490	Vis	0.110	1.5	13	44	Inf
		NIR	0.155	1.0	9.6	34	Inf
	677	Vis	1.2	58	Inf	–	–
		NIR	1.7	61	Inf	–	–
Aggregated monomers	490	Vis	0.085	0.68	3.0	17	142
		NIR	0.112	0.513	3.0	21	183
	677	Vis	1.1	19	118	–	–
		NIR	1.2	26	188	–	–
Trimers	490	Vis	0.101	0.603	4.1	20.8	Inf
		NIR	0.105	0.479	3.0	19	Inf
	677	Vis	1.2	14	Inf	–	–
		NIR	1.2	17	Inf	–	–
Aggregated trimers	490	Vis	0.088	0.412	1.5	16	124
		NIR	0.119	0.420	1.9	14	157
	677	Vis	1	15	144	–	–
		NIR	0.860	17	151	–	–

Uncertainties in the values based on the goodness of fit amount to no more than 10 % in all cases

further energy transfer from the carotenoids to Chl *b* is taking place, but that energy transfer to Chl *a* is occurring from either the carotenoids or Chl *b* or both. This second EADS component also shows a large, broad, positive feature between 500 and 600 nm that can be attributed to the buildup of excited state population in the S_1 state of the carotenoids via deactivation of the S_2 state in ≤155 fs. From previous work (Fuciman et al. 2012) this broad feature can be assigned to a vibronically hot $S_1 \rightarrow S_N$ transition of the carotenoids.

As the second EADS component decays to form the third EADS component, the amplitude of the broad positive feature between 500 and 600 nm remains relatively constant, but the width of the band narrows (see the green traces in the left hand column panels in Fig. 11). This change is accompanied by a further reduction in the magnitude of the bleaching of the Chl *b* Q_Y band, but a continued rise in the extent of bleaching of the Chl *a* Q_Y band. The narrowing of the $S_1 \rightarrow S_N$ transition of the carotenoid is very likely due to relaxation of the vibrationally hot S_1 state of the carotenoids (Billsten et al. 2002). Because the magnitude of this band is not changing very much, the additional bleaching of the Chl *a* Q_Y band that occurs can be accounted for by energy transfer from Chl *b* to Chl *a*.

In going from the third to the fourth EADS component (purple traces in the left hand column panels of Fig. 11), there is a significant reduction in the positive amplitude attributable to the $S_1 \rightarrow S_N$ excited state absorption of the carotenoids. Yet, only a very small increase in the amplitude associated with the bleaching of the Q_Y band of Chl *a* is seen, and this can be correlated with the disappearance of the bleaching of the Q_Y band of Chl *b*. This argues that

no further energy transfer from the carotenoids to Chl *a* is taking place, but Chl *b* is transferring all of its remaining excited state energy to Chl *a* in this time domain. Moreover, this observation strongly suggests that the S_1 state of the carotenoids is not involved in transferring energy to Chl *a* (Connelly et al. 1997). This is because the lifetime of the third EADS components is very similar to the S_1 lifetime reported for the carotenoids in LHCII complexes (Croce et al. 2001; Fuciman et al. 2012).

The fourth EADS component has a lifetime between 16 and 44 ps, and it decays into the final EADS component (blue traces in the left hand column panels of Fig. 11). The most notable spectral change accompanying this decay is that in all of the samples except the unaggregated monomeric LHCII complex, there is a profound decrease in the bleaching of the Q_Y band of Chl *a*. In the unaggregated monomeric LHCII complex, there is no change in the magnitude of the bleaching of this band in going from the fourth to the final EADS trace (see the purple and blue lines in the top left hand panel in Fig. 11). Also, the lifetime of the final EADS component is very long (infinite) for the unaggregated samples, but much faster at 142 and 124 ps for the aggregated monomers and aggregated trimers, respectively.

The EADS lineshapes resulting from a fit of the transient data taken using 677 nm are shown in the right hand column panels of Fig. 11. In all cases, three kinetic components were required to fit the data. Whereas the first two kinetic components have reasonably similar lifetimes for all the samples, there is a major difference in the lifetime of the third and final component. The lifetime of this component for the unaggregated monomers and trimers is

essentially infinite (non-decaying). However, as was evident in the fits to the data taken using 490 nm excitation (left hand column panels of Fig. 11), the lifetime of this final component decreases significantly upon aggregation of the LHCII complexes and becomes 118 ps for the monomers and 144 ps for the trimers. These results together with those obtained from the global fitting analysis of the data recorded using 490 nm excitation described above, clearly demonstrate that aggregation of either monomeric or trimeric LHCII complexes accelerates the decay of Chl a excited states.

The striking reduction in fluorescence intensity upon aggregation of the monomeric and trimeric LHCII complexes (Fig. 3) is highly suggestive of the formation of a quenching center (or centers) that facilitates deactivation of Chl a excited states. This idea is reinforced by the emission spectra of the aggregated LHCII samples taken at cryogenic temperatures (bottom two panels in Fig. 4) which show red-shifted (low-energy) fluorescence bands not seen in the spectra of purified Chl a and b (Fig. 5) nor in those from unaggregated LHCII complexes (top two panels in Fig. 4). The structure of the LHCII trimer (Liu et al. 2004) and previous work based on spectroscopy and mutagenesis

(Zucchelli et al. 1990; Trinkunas et al. 1997; Pieper et al. 1999a, b; Remelli et al. 1999; Rogl et al. 2002; Croce et al. 2003) suggest which Chls may be involved in the formation of these low-energy quenching centers.

It is very challenging to try to gain some insight into which specific protein-bound Chl molecules may be giving rise to the spectral differences that occur upon aggregation. Nevertheless, Gaussian deconvolution in the Q_Y region was carried out on the 10 K absorption spectra from aggregated and unaggregated monomeric and trimeric LHCII complexes (Fig. 12). The figure reveals that a large number of individual Chl a and b spectra having various amplitudes and widths are required to simulate the experimental absorption spectral lineshapes. However, it is clear that only some of the peaks have shifted or changed intensity upon aggregation. Difference spectra generated by subtracting the spectra of the unaggregated complexes from those of the aggregated complexes reveal that the major change in the lineshapes upon aggregation occurs on the low-energy side of the Q_Y band of Chl a. Gaussian components 1 and 2 from the trimers undergo a red-shift of 2 nm. The spectral shifts of all the other Gaussian components induced by aggregation of either the monomers or
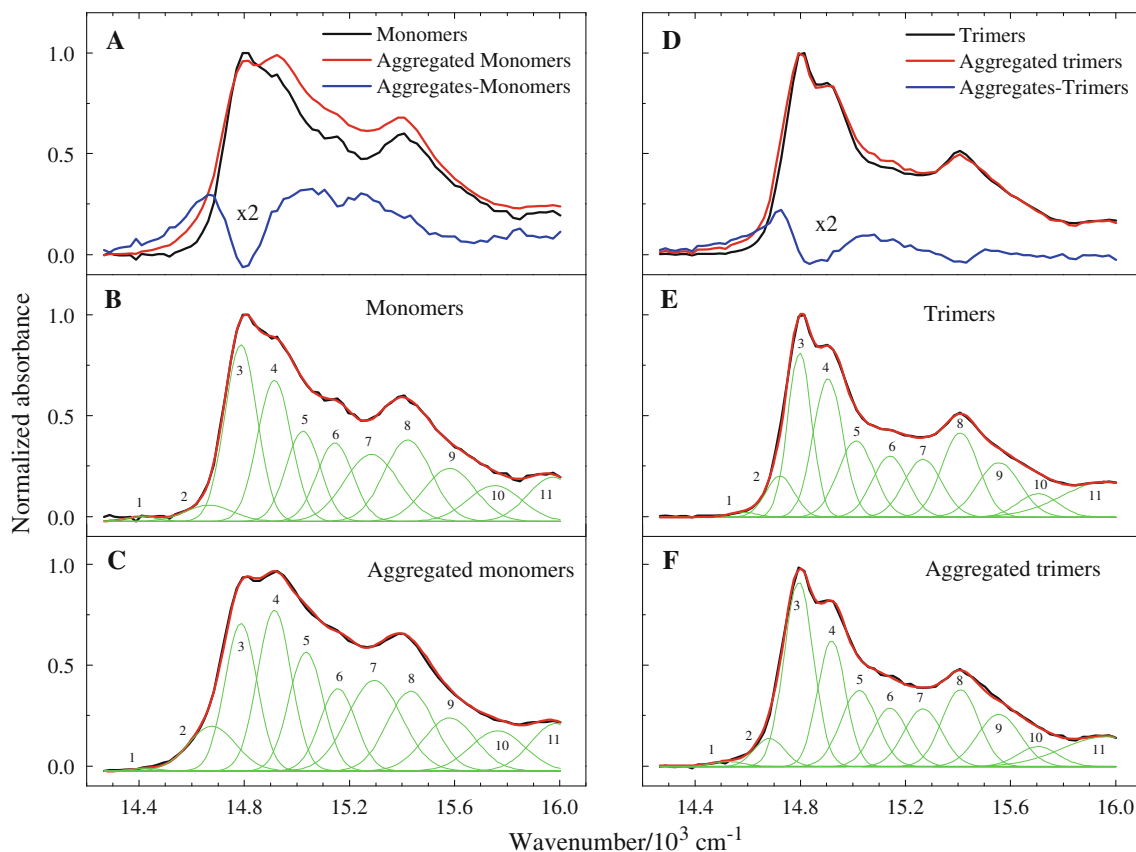

Fig. 12 Gaussian fits of the 10 K steady-state absorption spectra of unaggregated and aggregated LHCII monomers and trimers. The parameters used in the fits are summarized in Table 2

trimers is only 1 nm. Aggregation of the monomeric LHCII complex leads to an increase in the amplitude of the Chl *a* spectral component (Gaussian peak 2) having a maximum at 682 nm (14,660 cm^{-1}) and a decrease in the amplitude of the Chl *a* spectral component (Gaussian peak 3) having a maximum at 676 nm (14,790 cm^{-1}), while aggregation of the trimeric LHCII complex leads to a decrease in the amplitude of the Chl *a* spectral component (Gaussian peak 2) having a maximum at 679 nm (14,720 cm^{-1}) and an increase in the amplitude of the Chl *a* spectral component (Gaussian peak 3) having a maximum at 676 nm (14,800 cm^{-1}) (see Table 2 for a summary of all the Gaussian fitting parameters). For the aggregated monomers, the decrease in peak 3 leads to a pronounced dip in a broad positive band formed from small increases in the amplitudes of several other Chl absorption bands (Fig. 12a). This broad positive band in the difference spectrum is much less evident upon aggregation of the trimers (Fig. 12d). These results suggest that the Chl

a molecules associated with the red-most absorption bands in the unaggregated complexes are the ones most affected by aggregation. It remains to be demonstrated that these are the Chls involved in fluorescence quenching. If this was the case, one would expect to see agreement between the spectra of one or more of the fast-decaying fluorescence kinetic components shown in Fig. 8 and the red-shifted fluorescence peaks appearing in the spectra of the aggregated LHCII complexes (Fig. 4). For both monomeric and trimeric samples, aggregation leads to a very noticeable increase in intensity and red-shift in the spectrum of the fastest fluorescence decay component recorded at room temperature (see the square symbols in Fig. 8), but the relatively low-resolution steady-state fluorescence spectra taken at room temperature precludes a precise assignment of the maximum in the red-shifted peak.

Remelli et al. (1999) proposed on the basis of site-directed mutagenesis of pigment-binding residues in recombinant, pigment-reconstituted, refolded monomeric

Table 2 Parameters from the Gaussian fits to the absorption spectra of LHCII monomers, trimers, and aggregates shown in Fig. 12

Peak	Monomers					Aggregated monomers				
	Center of gravity (cm^{-1})	Wavelength (nm)	Maximum height	Peak area	FWHM (cm^{-1})	Center of gravity (cm^{-1})	Wavelength (nm)	Maximum height	Peak area	FWHM (cm^{-1})
1	14,410	694	0.0241	3.512	138	14,420	693	0.0143	2.106	139
2	14,660	682	0.0810	18.30	212	14,680	681	0.2218	50.12	212
3	14,790	676	0.8763	134.6	144	14,790	676	0.7316	112.4	144
4	14,920	670	0.7013	112.4	151	14,920	670	0.7981	128.0	151
5	15,020	666	0.4473	72.82	153	15,040	665	0.5901	96.067	153
6	15,140	660	0.3886	66.65	161	15,160	660	0.4085	70.06	161
7	15,280	654	0.3323	85.26	241	15,300	654	0.4491	115.2	241
8	15,420	648	0.4041	90.68	211	15,430	648	0.3951	88.66	211
9	15,580	642	0.2630	64.41	230	15,580	642	0.2625	64.29	230
10	15,750	635	0.1780	45.04	239	15,760	634	0.1993	50.29	239
11	15,970	626	0.2193	32.21	223	15,980	626	0.2348	31.88	223

Peak	Trimers					Aggregated trimers				
	Center of gravity (cm^{-1})	Wavelength (nm)	Maximum height	Peak area	FWHM (cm^{-1})	Center of gravity (cm^{-1})	Wavelength (nm)	Maximum height	Peak area	FWHM (cm^{-1})
1	14,580	686	0.0239	3.241	127	14,530	688	0.0232	3.305	134
2	14,720	679	0.2037	27.64	127	14,680	681	0.1399	19.90	134
3	14,800	676	0.8154	92.91	107	14,790	676	0.9153	128.2	132
4	14,900	671	0.6878	96.66	132	14,920	670	0.6241	83.22	125
5	15,010	666	0.3777	65.18	162	15,020	666	0.3780	65.18	162
6	15,140	660	0.3033	51.31	159	15,140	660	0.2897	49.00	159
7	15,270	655	0.2872	51.77	169	15,270	655	0.2872	51.77	169
8	15,410	649	0.4192	73.48	165	15,410	649	0.3818	66.93	165
9	15,560	643	0.2700	55.11	192	15,560	643	0.2592	52.91	192
10	15,700	637	0.1163	22.15	179	15,710	637	0.0989	18.83	179
11	15,960	626	0.1752	43.31	388	15,960	627	0.1472	36.38	388

LHCII that Chl A2 (denoted *a*612 in Fig. 1b) accounted for 75 % of the absorption at 681 nm, that it was the chromophore with the lowest energy in LHCII, and consequently represented an important avenue for energy transfer to neighboring antenna proteins. These authors also suggested that three other Chl molecules, A1, A6, and B1, denoted Chl *a*610, *a*604, and *b*608 in the notation of Liu et al. (2004) (Fig. 1), and Chls 1, 6, and 11 in the notation of Standfuss et al. (2005), contribute to the low-energy absorption band at 681 nm for the monomers (Remelli et al. 1999). Subsequently, Rogl et al. (2002) argued from similar studies on trimeric complexes that Chl *a*612, denoted Chl a2 by these authors, but absorbing at 676 nm in the trimers rather than at 681 nm for the monomeric LHCII, represented the terminal state in the energy transfer pathway of LHCII as suggested by Remelli et al. (1999). However, definitive assignment of the individual Chl molecules in the LHCII structure to specific spectral features on the basis of mutagenesis and/or pigment reconstitution is complicated by the fact that changing the environment of one Chl may affect the spectrum of another. Nevertheless, subsequent experimental work and modeling revealed the details of the interactions between the pigments, and that Chls *a*610, *a*611, and *a*612 (Fig. 1b) represented the lowest energy emitters in LHCII (van Grondelle and Novoderezhkin 2006; Georgakopoulou et al. 2007). These Chls are in close contact with lutein 1 (Fig. 1b) which has been reported to undergo a distortion during the transition of LHCII into the quenched state (Johnson and Ruban 2009; Ilioaia et al. 2011b). It was also shown that isolated LHCII complexes immobilized in a gel matrix display the same spectral characteristics as seen for LHCII aggregates (Ilioaia et al. 2011b). This work also supported the proposal that spectral changes in the bands associated with Chls *a*610, *a*611, and *a*612 are indicative of an altered protein environment that enhances energy transfer to the S_1 excited state of lutein 1 as the quenching site (Pascal et al. 2005; Ruban et al. 2007; Wahadoszamen et al. 2012). In other studies, it was shown that different crystal forms of trimeric LHCII display different extents of fluorescence quenching, which supports a model for quenching that involves protein conformational changes within trimers (van Oort et al. 2011). Thus, it is apparent that not only aggregation of the LHCII complex, the effects of which are detailed in the present study, but other perturbations that cause protein structural changes, can alter the absorption and fluorescence spectral profiles of the bound pigments, modulate their energy transfer and fluorescence kinetics, and result in the dissipation of a large portion of the absorbed light energy.

References

Ahn TK, Avenson TJ, Ballottari M, Cheng YC, Niyogi KK, Bassi R, Fleming GR (2008) Architecture of a charge-transfer state regulating light harvesting in a plant antenna protein. Science 320:794–797

Amarie S, Standfuss J, Barros T, Külbrandt W, Dreuw A, Wachtveitl J (2007) Carotenoid radical cations as a probe for the molecular mechanism of nonphotochemical quenching in oxygenic photosynthesis. J Phys Chem B 111:3481–3487

Andersson J, Walters RG, Horton P, Jansson S (2001) Antisense inhibition of the photosynthetic antenna proteins CP29 and CP26: implications for the mechanism of protective energy dissipation. Plant Cell 13:1193–1204

Andreeva A, Abarova S, Stoitchkova K, Busheva M (2009) Model for fluorescence quenching in light harvesting complex II in different aggregation states. Eur Biophys J 38:199–208

Avenson TJ, Ahn TK, Zigmantas D, Niyogi K, Li Z, Ballottari M, Bassi R, Fleming GR (2008) Zeaxanthin radical cation formation in minor light-harvesting complexes of higher plant antenna. J Biol Chem 283:3550–3558

Avenson TJ, Ahn TK, Niyogi KK, Ballottari M, Bassi R, Fleming GR (2009) Lutein can act as a switchable charge transfer quencher in the CP26 light-harvesting complex. J Biol Chem 284:2830–2835

Barros T, Kuhlbrandt W (2009) Crystallisation, structure and function of plant light-harvesting complex II. Biochim Biophys Acta 1787:753–772

Barros T, Royant A, Standfuss J, Dreuw A, Kuhlbrandt W (2009) Crystal structure of plant light-harvesting complex shows the active, energy-transmitting state. EMBO J 28:298–306

Barzda V, Gulbinas V, Kananavicius R, Cervinskas V, Van Amerongen H, Van Grondelle R, Valkunas L (2001) Singlet-singlet annihilation kinetics in aggregates and trimers of LHCII. Biophys J 80:2409–2421

Bassi R, Silvestri M, Dainese P, Moya I, Giacometti G (1991) Effects of a non-ionic detergent on the spectral properties and aggregation state of the light-harvesting chlorophyll *a/b* protein complex (LHCII). J Photochem Photobiol B 9:335–354

Berthold DA, Babcock GT, Yocum CF (1981) A highly resolved, oxygen-evolving photosystem II preparation from spinach thylakoid membranes. FEBS Lett 134:231–234

Billsten HH, Zigmantas D, Sundström V, Polívka T (2002) Dynamics of vibrational relaxation in the S_1 state of carotenoids having 11 conjugated C=C bonds. Chem Phys Lett 355:465–470

Blankenship RE (2002) Molecular mechanisms of photosynthesis. Blackwell Science, Oxford

Bode S, Quentmeier CC, Liao P-N, Barros T, Walla PJ (2008) Xanthophyll-cycle dependence of the energy transfer between carotenoid dark states and chlorophylls in NPQ mutants of living plants and in LHC II. Chem Phys Lett 450:379–385

Bode S, Quentmeier CC, Liao P-N, Hafi N, Barros T, Wilk L, Bittner F, Walla PJ (2009) On the regulation of photosynthesis by excitonic interactions between carotenoids and chlorophylls. Proc Natl Acad Sci USA 106:12311–12316

Cheng Y-C, Ahn T-K, Avenson TJ, Zigmantas D, Niyogi KK, Ballottari M, Bassi R, Fleming GR (2008) Kinetic modeling of charge-transfer quenching in the CP29 minor complex. J Phys Chem B 112:13418–13423

Connelly JP, Mueller MG, Bassi R, Croce R, Holzwarth AR (1997) Femtosecond transient absorption study of carotenoid to

chlorophyll energy transfer in the light-harvesting complex II of photosystem II. Biochemistry 36:281–287

Croce R, Weiss S, Bassi R (1999) Carotenoid-binding sites of the major light-harvesting complex II of higher plants. J Biol Chem 274:29613–29623

Croce R, Muller MG, Bassi R, Holzwarth AR (2001) Carotenoid-to-chlorophyll energy transfer in recombinant major light-harvesting complex (LHCII) of higher plants. I Femtosecond transient absorption measurements. Biophys J 80:901–915

Croce R, Muller MG, Caffari S, Bassi R, Holzwarth AR (2003) Energy transfer pathways in the minor antenna complex CP29 of photosystem II: a femtosecond study of carotenoid to chlorophyll transfer in mutant and WT complexes. Biophys J 84:2517–2532

Das SK, Frank HA (2002) Pigment compositions, spectral properties, and energy transfer efficiencies between the xanthophylls and chlorophylls in the major and minor pigment–protein complexes of photosystem II. Biochemistry 41:13087–13095

Demmig-Adams B, Adams WWI (1992) Photoprotection and other responses of plants to high light stress. Annu Rev Plant Physiol Mol Biol 43:599–626

Demmig-Adams B, Adams WW (2002) Antioxidants in photosynthesis and human nutrition. Science 298:2149–2153

Foote CS (1968) Mechanisms of photosensitized oxidation. Science 162:963–970

Foote CS, Chang YC, Denny RW (1970) Chemistry of singlet oxygen. X. Carotenoid quenching parallels biological protection. J Am Chem Soc 92:5216–5218

Foyer C, Harbinson J (1999) Relationships between antioxidant metabolism and carotenoids in the regulation of photosynthesis. In: Frank HA, Young AJ, Britton G, Cogdell RJ (eds) The photochemistry of carotenoids, vol 8., Advances in photosynthesisKluwer Academic Publishers, Dordrecht, pp 305–325

Frank HA, Cogdell RJ (1996) Carotenoids in photosynthesis. Photochem Photobiol 63:257–264

Frank HA, Cogdell RJ (2012) Light capture in photosynthesis. In: Egelman EH (ed) Comprehensive biophysics, vol 8. Academic Press, Oxford, pp 94–114

Frank HA, Das SK, Bautista JA, Bruce D, Vasilev S, Crimi M, Croce R, Bassi R (2001) Photochemical behavior of xanthophylls in the recombinant photosystem II antenna complex, CP26. Biochemistry 40:1220–1225

Fromme P, Mathis P (2004) Unraveling the photosystem I reaction center: a history, or the sum of many efforts. Photosynth Res 80:109–124

Fuciman M, Enriquez MM, Polivka T, Dall'Osto L, Bassi R, Frank HA (2012) Role of xanthophylls in light harvesting in green plants: a spectroscopic investigation of mutant LHCII and Lhcb pigment–protein complexes. J Phys Chem B 116:3834–3849. doi:10.1021/jp210042z

Georgakopoulou S, van der Zwan G, Bassi R, van Grondelle R, van Amerongen H, Croce R (2007) Understanding the changes in the circular dichroism of light harvesting complex II upon varying its pigment composition and organization. Biochemistry 46:4745–4754

Gilmore AM, Hazlett TL, Govindjee (1995) Xanthophyll cycle-dependent quenching of photosystem II chlorophyll a fluorescence: formation of a quenching complex with a short fluorescence lifetime. Proc Natl Acad Sci USA 92:2273–2277

Gradinaru CC, van Stokkum IHM, Pascal AA, van Grondelle R, van Amerongen H (2000) Identifying the pathways of energy transfer between carotenoids and chlorophylls in LHCII and CP29. A multicolor, femtosecond pump-probe study. J Phys Chem B 104:9330–9342

Green BR, Parson WW (2003) Light-harvesting antennas in photosynthesis, vol 13. In: Advances in photosynthesis and respiration. Kluwer Academic Publishers, Dordrecht

Gruszecki WI, Grudzinski W, Gospodarek M, Patyra M, Maksymiec W (2006) Xanthophyll-induced aggregation of LHCII as a switch between light-harvesting and energy dissipation systems. Biochim Biophys Acta 1757:1504–1511

Gruszecki WI, Luchowski R, Grudzinski W, Gryczynski I (2012) Photosynthetic antenna complex LHCII studied with novel fluorescence techniques. In: Bujalowski WM (ed) Spectroscopic methods of analysis: methods and protocols, vol 875., Methods in molecular biologySpringer Science, New York, pp 263–269

Hofmann E, Wrench PM, Sharples FP, Hiller RG, Welte W, Diederichs K (1996) Structural basis of light harvesting by carotenoids: Peridinin–chlorophyll–protein from Amphidinium carterae. Science 272:1788–1791

Holt NE, Fleming GR, Niyogi KK (2004) Toward an understanding of the mechanism of nonphotochemical quenching in green plants. Biochemistry 43:8281–8289

Holt NE, Zigmantas D, Valkunas L, Li XP, Niyogi KK, Fleming GR (2005) Carotenoid cation formation and the regulation of photosynthetic light harvesting. Science 307:433–436

Holzwarth AR, Miloslavina Y, Nilkens M, Jahns P (2009) Identification of two quenching sites active in the regulation of photosynthetic light-harvesting studied by time-resolved fluorescence. Chem Phys Lett 483:262–267

Horton P, Ruban A (2005) Molecular design of the photosystem II light-harvesting antenna: photosynthesis and photoprotection. J Exp Bot 56:365–373

Horton P, Ruban AV, Walters RG (1996) Regulation of light harvesting in green plants. Annu Rev Plant Physiol Mol Biol 47:655–684

Horton P, Ruban AV, Young AJ (1999) Regulation of the structure and function of the light harvesting complexes of photosystem II by the xanthophyll cycle. In: Frank HA, Young AJ, Britton G, Cogdell RJ (eds) The photochemistry of carotenoids, vol 8. Advances in photosynthesis. Kluwer Academic Publishers, Dordrecht, pp 271–291

Huyer J, Eckert H-J, Irrgang K-D, Miao J, Eichler H-J, Renger G (2004) Fluorescence decay kinetics of solubilized pigment protein complexes from the distal, proximal, and core antenna of photosystem II in the range of 10–277 K and absence or presence of sucrose. J Phys Chem B 108:3326–3334

Ide JP, Klug DR, Kühlbrandt W, Giorgi LB, Porter G (1987) The state of detergent solubilised light-harvesting chlorophyll-a/b protein complex as monitored by picosecond time-resolved fluorescence and circular dichroism. Biochim Biophys Acta 893:349–364

Ilagan RP, Christensen RL, Chapp TW, Gibson GN, Pascher T, Polivka T, Frank HA (2005) Femtosecond time-resolved absorption spectroscopy of astaxanthin in solution and in α-crustacyanin. J Phys Chem A 109:3120–3127

Ilioaia C, Johnson MP, Duffy CDP, Pascal AA, van Grondelle R, Robert B, Ruban AV (2011a) Origin of absorption changes associated with photoprotective energy dissipation in the absence of zeaxanthin. J Biol Chem 286:91–98

Ilioaia C, Johnson MP, Liao P-N, Pascal AA, van Grondelle R, Walla PJ, Ruban AV, Robert B (2011b) Photoprotection in plants involves a change in lutein 1 binding domain in the major light-harvesting complex of photosystem II. J Biol Chem 286:27247–27254

Johnson MP, Ruban AV (2009) Photoprotective energy dissipation in higher plants involves alteration of the excited state energy of the emitting chlorophyll(s) in the light harvesting antenna II (LHCII). J Biol Chem 284:23592–23601

Krieger-Liszkay A (2004) Singlet oxygen production in photosynthesis. J Exp Bot 56:337–346

Kühlbrandt W, Wang DN, Fujiyoshi Y (1994) Atomic model of plant light-harvesting complex by electron crystallography. Nature 367:614–621

Kulheim C, Agren J, Jansson S (2002) Rapid regulation of light harvesting and plant fitness in the field. Science 297:91–93

Liao PN, Bode S, Wilk L, Hafi N, Walla PJ (2010) Correlation of electronic carotenoid–chlorophyll interactions and fluorescence quenching with the aggregation of native LHC II and chlorophyll deficient mutants. Chem Phys 373:50–55

Liu ZF, Yan HC, Wang KB, Kuang TY, Zhang JP, Gui LL, An XM, Chang WR (2004) Crystal structure of spinach major light-harvesting complex at 2.72 Å resolution. Nature 428:287–292

Miloslavina Y, Wehner A, Lambrev PH, Wientjes E, Reus M, Garab G, Croce R, Holzwarth AR (2008) Far-red fluorescence: a direct spectroscopic marker for LHCII oligomer formation in non-photochemical quenching. FEBS Lett 582:3625–3631

Moya I, Silvestri M, Vallon O, Cinque G, Bassi R (2001) Time-resolved fluorescence analysis of the photosystem II antenna proteins in detergent micelles and liposomes. Biochemistry 40:12552–12561

Mozzo M, Dall'Osto L, Hienerwadel R, Bassi R, Croce R (2008) Photoprotection in the antenna complexes of photosystem II. Role of individual xanthophylls in chlorophyll triplet quenching. J Biol Chem 283:6184–6192

Muller MG, Lambrev P, Reus M, Wientjes E, Croce R, Holzwarth AR (2010) Singlet energy dissipation in photosystem II light-harvesting complex does not involve energy transfer to carotenoids. ChemPhysChem 11:1289–1296

Müller P, Li X-P, Niyogi KK (2001) Non-photochemical quenching. A response to excess light energy. Plant Physiol 125:1566–1588

Mullineaux CW, Pascal AA, Horton P, Holzwarth AR (1993) Excitation-energy quenching in aggregates of the LHC II chlorophyll–protein complex: a time-resolved fluorescence study. Biochim Biophys Acta 1141:23–28

Naqvi KR, Melo TB, Raju BB, Javorfi T, Simidjiev I, Garab G (1997) Quenching of chlorophyll a singlets and triplets by carotenoids in light-harvesting complex of photosystem II: comparison of aggregates with trimers. Spectrochim Acta A 53:2659–2667

Nelson N, Yocum CF (2006) Structure and function of photosystems I and II. Annu Rev Plant Biol 57:521–565

Niyogi K, Li X-P, Rosenberg V, Jung H-S (2005) Is PsbS the site of non-photochemical quenching in photosynthesis? J Exp Bot 56:375–382

Nordlund TM (1981) Lifetime of fluorescence from light-harvesting chlorophyll a/b proteins excitation intensity dependence. Biophys J 36:193–201

Palacios MA, de Weerd FL, Ihalainen JA, van Grondelle RV, Amerongen HV (2002) Superradiance and exciton (de)localization in light-harvesting complex II from green plants? J Phys Chem B 106:5782–5787

Pascal AA, Liu Z, Broess K, van Oort B, van Amerongen H, Wang C, Horton P, Robert B, Chang W, Ruban AV (2005) Molecular basis of photoprotection and control of photosynthetic light-harvesting. Nature 436:134–137

Peter GF, Thornber JP (1991) Biochemical composition and organization of higher plant photosystem II light harvesting pigment proteins. J Biol Chem 266:16745–16754

Phillip D, Ruban AV, Horton P, Asato A, Young AJ (1996) Quenching of chlorophyll fluorescence in the major light-harvesting complex of photosystem II: a systematic study of the effect of carotenoid structure. Proc Natl Acad Sci USA 93:1492–1497

Pieper J, Irrgang K-D, Rätsep M, Jankowiak R, Schrötter T, Voigt J, Small GJ, Renger G (1999a) Effects of aggregation on trimeric light-harvesting complex II of green plants: a hole-burning study. J Phys Chem A 103:2422–2428

Pieper J, Rätsep M, Jankowiak R, Irrgang K-D, Voigt J, Renger G, Small GJ (1999b) Q_Y-level structure and dynamics of solubilized

light-harvesting complex II of green plants: pressure and hole burning studies. J Phys Chem A 103:2412–2421

Remelli R, Varotto C, Sandona D, Croce R, Bassi R (1999) Chlorophyll binding to monomeric light-harvesting complex. J Biol Chem 274:33510–33521

Rogl H, Schödel R, Lokstein H, Kühlbrandt W, Schubert A (2002) Assignment of spectral substructures to pigment-binding sites in higher plant light-harvesting complex LHC-II. Biochemistry 41:2281–2287

Roszak AW, Howard TD, Southall J, Gardiner AT, Law CJ, Isaacs NW, Cogdell RJ (2003) Crystal structure of the RC-LH1 core complex from Rhodopseudomonas palustris. Science 302:1969–1972

Ruban AV, Dekker JP, Horton P, van Grondelle R (1995) Temperature dependence of chlorophyll fluorescence from the light harvesting complex II of higher plants. Photochem Photobiol 61:216–221

Ruban AV, Young AJ, Horton P (1996) Dynamic properties of the minor chlorophyll a/b binding proteins of photosystem II, an in vitro model for photoprotective energy dissipation in the photosynthetic membrane of green plants. Biochemistry 35:674–678

Ruban AV, Calkoen F, Kwa SLS, van Grondelle R, Horton P, Dekker JP (1997) Characterisation of LHCII in the aggregated state by linear and circular dichroism spectroscopy. Biochim Biophys Acta 1321:61–70

Ruban AV, Lee PJ, Wentworth M, Young AJ, Horton P (1999) Determination of the stoichiometry and strength of binding of xanthophylls to the photosystem II light harvesting complexes. J Biol Chem 274:10458–10465

Ruban AV, Berera R, Ilioaia C, van Stokkum IHM, Kennis JTM, Pascal AA, van Amerongen H, Robert B, Horton P, van Grondelle R (2007) Identification of a mechanism of photoprotective energy dissipation in higher plants. Nature 450:575–579

Standfuss J, van Scheltinga ACT, Lamborghini M, Külbrandt W (2005) Mechanisms of photoprotection and nonphotochemical quenching in pea light harvesting complex at 2.5A resolution. EMBO J 24:919–928

Telfer A, Pascal A, Gall A (2008) Carotenoids in photosynthesis. In: Britton G, Liaaen-Jensen S, Pfander H (eds) Carotenoids: natural functions, vol 4. Birkäuser Verlag, Basel

Trinkunas G, Connelly JP, Müller MG, Valkunas L, Holzwarth AR (1997) Model for the excitation dynamics in the light-harvesting complex II from higher plants. J Phys Chem B 101:7313–7320

van Grondelle R, Novoderezhkin VI (2006) Energy transfer in photosynthesis: experimental insights and quantitative models. Phys Chem Chem Phys 8:793–807

van Oort B, van Hoek A, Ruban AV, van Amerongen H (2007) Equilibrium between quenched and nonquenched conformations of the major plant light-harvesting complex studied with high-pressure time-resolved fluorescence. J Phys Chem B 111:7631–7637

van Oort B, Maréchal A, Ruban AV, Robert B, Pascal AA, de Ruijter NCA, van Grondelle R, van Amerongen H (2011) Different crystal morphologies lead to slightly different conformations of light-harvesting complex II as monitored by variations of the intrinsic fluorescence lifetime. Phys Chem Chem Phys 13:12614–12622

van Stokkum IHM, Larsen DS, van Grondelle R (2004) Global and target analysis of time-resolved spectra. Biochim Biophys Acta 1657:82–104

Vasil'ev S, Irrgang K-D, Schrötter T, Bergmann A, Eichler H-J, Renger G (1997) Quenching of chlorophyll a fluorescence in the aggregates of LHCII: steady state fluorescence and picosecond relaxation kinetics. Biochemistry 36:7503–7512

Wahadoszamen M, Berera R, Ara AM, Romero E, van Grondelle R (2012) Identification of two emitting sites in the dissipative state of the major light harvesting antenna. Phys Chem Chem Phys 14:759–766

Witt HT, Witt I, Krauss N, Hinrichs W, Fromme P, Saenger W (1994) Crystals and structure of photosystem-1. Biophys J 66:A2

Zucchelli G, Jennings RC, Garlaschi FM (1990) The presence of long-wavelength chlorophyll *a* spectral forms in the light-harvesting chlorophyll *a/b* protein complex II. J Photochem Photobiol B 6:381–394